



Analysis and Perspective of Thermal Interface Material Properties Under High Power Density Operating Conditions

Chaoyue Liu, Cheng Ruan, Long Sun, Yaowei Huang,
Yang Wang and Yu Cui

EasyChair preprints are intended for rapid
dissemination of research results and are
integrated with the rest of EasyChair.

July 1, 2024

ANALYSIS AND PERSPECTIVE OF THERMAL INTERFACE MATERIAL PROPERTIES UNDER HIGH POWER DENSITY OPERATING CONDITIONS

Chaoyue Liu¹, Cheng Ruan¹, Long Sun¹, Yaowei Huang¹, Yang Wang^{1,2}, Yu Cui¹

(1.Changchun Cedar Electronics Technology Co., Ltd., Changchun 130103, China; 2.Changchun Institute of Optics, Fine Mechanics and Physics, Chinese Academy of Sciences, Changchun 130103, China)

ABSTRACT

With the integration of electronic devices, the continuous increase in power density, the emergence of high-power LEDs, and the continuation of Moore's Law, miniaturization of electronic product feature sizes inevitably leads to increased power density of electronic devices. Therefore, thermal conduction is gradually becoming a limiting factor in improving feature density. Due to the existence of contact thermal resistance between heating devices and heat dissipation structures, thermal interface materials are required to fill in order to reduce contact thermal resistance and enhance thermal conduction efficiency and pathways between materials interfaces. This paper investigates and experimentally measures three commonly used types of thermal interface materials—metallic solder, pads, and gels. It compares and analyzes the processing techniques, filling effects, and performance testing of 11 interface material samples. The results indicate that under conditions of a 500W high-power COB LED light source, four samples show superior thermal conductivity compared to thermal grease as the baseline. For metallic solder, the duration and temperature settings of each temperature zone in the process, as well as the environment inside the soldering furnace, significantly affect the soldering results. Improving the soldering process flow and adjusting the duration of each part of the process enhance soldering effects and reduce solder void rates. Process adjustments and improvements notably enhance soldering effects. Meeting the heat conduction needs of high-power and high-power density device thermal sources holds promising prospects for future applications in heat dissipation for high-power density devices.

Keywords: Thermal interface materials, COB LEDs, Contact thermal resistance, Performance analysis, Recommendations

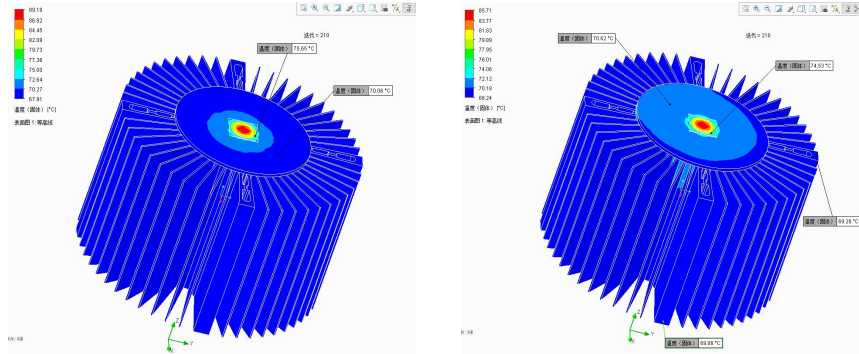
1. INTRODUCTION

As technology continues to advance, electronic devices are becoming increasingly dense, integrated, and compact, leading to a significant concentration of heat generation. As the fourth-generation solid-state lighting source, Light Emitting Diodes (LEDs) offer advantages such as energy efficiency, environmental friendliness, safety, reliability, longevity, low power consumption, and high brightness[1,2]. However, only about 20% of the energy consumed by LEDs is used for illumination, while approximately 70% is converted into heat[3-6]. The heat generated must be transferred from the heat source to the cooling components, with effective heat dissipation being essential for temperature control. Efficiently transferring heat from the heat source to the cooling component is a key challenge for centralized heat sources. The surfaces between heating and cooling devices are often uneven, preventing tight contact. The air gaps at these contact surfaces result in extremely low efficiency of heat transfer from the heating device to the cooling component. Consequently, a substantial amount of heat accumulates at the heat source, leading to high temperatures that can adversely affect the quality and lifespan of the heat source.

Based on the aforementioned background, a detailed investigation of thermal interface materials (TIMs) was conducted. Commonly used TIMs include metal solder sheets, thermal greases, thermal pads, and thermal gels. The prevalent application processes are soldering and press-fitting. Through both research and practical measurements, the thermal conductivity and contact thermal resistance of each material were obtained. Additionally, the experimental soldering process provided a deeper and clearer understanding of the experiment procedural and necessary adjustments.

2. SIMULATION AND INVESTIGATION OF THERMAL INTERFACE MATERIAL PROPERTIES

Commonly used thermal interface materials (TIMs) currently include thermal grease, thermal pads, thermal gels, and metal solders. Using simulation software, the thermal conductivity of different interface materials was compared by monitoring the temperatures at the heat source, the radiator substrate and the radiator fins. The following figures evaluate the heat dissipation performance of thermal grease and metal solder sheets as thermal interface materials.



(a) Thermally conductive silicone grease 8.5W/m-K (b) Metal solder 83W/m-K

Figure 1. Simulation results of the performance of different thermally conductive interface materials

Simulation results indicate that when the thermal interface material is thermal grease, the temperature at the LED heat source is 89.2°C, with a temperature rise of 64.2°C. And, when the thermal interface material is a metal solder, the temperature at the LED heat source drops to 85.7°C, with a temperature rise of 60.7°C. These results demonstrate that using a thermal interface material with high thermal conductivity can effectively reduce the temperature at the heat source, ensuring safer and more efficient operation of the light source and the lamp components.

We explored the soldering and packaging processes between semiconductor light sources and heat dissipation substrates. By adjusting the duration, temperature, and furnace environment for each temperature zone based on soldering outcomes, we investigated the integrated packaging structure between the light source and the heat dissipation substrate. The choice of solder was based on parameters such as substrate material, roughness, and the maximum temperature the light source could withstand. The parameters of the solders are detailed in the Table 1:

Table 1. Summary of the research on the parameters of metal solders

serial number	Solder	melting point temperature (° C)	heat conductivity (W / (m · K))
1	In97Ag3 Solder	143	73
2	In52Sn48 Solder	118	34
3	Pb60In40 Solder	231	19
4	Sn96.5Ag3.5 Solder	221	33
5	Bi58Sn42 Solder	138	19
6	SAC305 Solder	218	58
7	Sn63Pb37 Solder	183	51
8	Low Temperature Solder PastePF-4258-C	138	19
9	High Temperature Solder PasteSAC305	218	58

The selection of metal solder sheets was based on the limitations encountered during use, material parameters, and preliminary testing of samples. During the soldering process, prolonged high temperatures in the reflow soldering furnace can negatively affect the LED light source chips. Therefore, it is crucial to ensure that the furnace temperature does not exceed the maximum tolerable temperature of the silicone surface of the light source. Additionally, it is important to ensure that the metal solder can melt between the heat sink's large heat capacity equalizing plate

and the light source substrate, while also selecting metal solder sheets with the highest possible thermal conductivity. By comparing the parameters of different metal solder sheets and conducting soldering experiments with two types of solder pastes, a suitable metal solder sheet was chosen based on the welding results and conclusions. After considering all factors, the In97Ag3 solder sheet was ultimately selected.

After determining the appropriate solder sheet, soldering was performed using a heating platform and a reflow soldering furnace. High temperatures were generated by the circulation of gas within the soldering machine to complete the welding process. The light source substrate, metal solder sheet, and heat sink equalizing plate were sequentially stacked and then pushed into the reflow soldering furnace to integrate the light source substrate, metal solder sheet, and heat sink equalizing plate into a unified assembly.

3. EXPERIMENTAL PROCEDURE, PERFORMANCE CONCLUSIONS AND ANALYSIS

After the integrated welding of the light source substrate, In97Ag3 solder, and heat spreader structure, an industrial CT scan was performed on the integrated structure comprising the heat source substrate, metal solder, and heat sink substrate. The scan revealed the melting and filling performance of the metal solder, which significantly affects the efficiency of heat transfer from the heat source. The better the filling performance, the more effectively the metal solder functions. The results of the industrial CT scan are shown in the Fig 2.

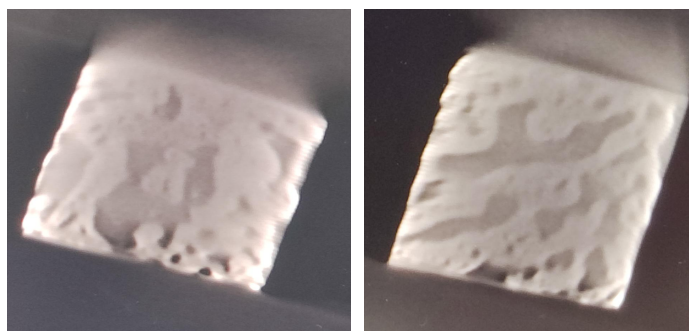


Figure 2. Soldering effect

After completing the industrial CT scan, the integrated structure was assembled with the main heat dissipation body of the heat sink. The processes of vacuum extraction, liquid filling, and pressing were then carried out to produce the prototype of the heat sink lamp. To evaluate the performance of the integrated thermal interface material structure, a temperature testing system was established. The prototype, power supply, K-type thermocouple, and Agilent data acquisition instrument were connected in sequence for performance testing. The diagram of the experimental setup after connection is shown in Fig 3.

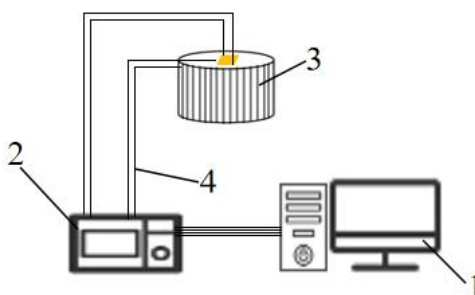


Figure 3. Diagram of the experimental system

1-Computer, 2-Data collector, 3-LED lighting radiator, 4-Type K thermocouple

Based on the established testing platform, we can meet all experimental needs for performance verification or testing of thermal interface materials and heat sinks. This platform supports the performance validation and related research of TIMs.

To verify the ability of various TIMs to reduce the thermal contact resistance between the light source substrate and the heat sink, experimental validation was conducted. Different TIMs were tested and compared by using the same specification light source and heat sink under identical

heating power. The resulting temperature rises with different TIMs were measured, reflecting their gap-filling capabilities and effectiveness in reducing contact thermal resistance.

A study was conducted on commonly used TIMs: metal solder, thermal grease, thermal pads, and thermal gels. We requested and tested 11 samples, including three metal solders, four thermal pads, two carbon fiber pads, and two thermal gels. The performance of these 11 TIM samples is detailed in the Table 2.

Table 2. Thermally conductive interface material parameters

	serial number	typology	Brinell hardness (HB)	heat conductivity (W/ (m·K))	the source	technique	
thermal interface material	sample 1	metal solders	111	73	home-made	soldered	
	sample 2		111	73			
	sample 3		108	86			
	sample 4	thermal pads	25	6		home-made	cladding
	sample 5		35	6			
	sample 6		25	8			
	sample 7		35	8			
	sample 8	carbon fiber spacer	12	12	inlet		
	sample 9		25	25			
	sample 10	thermal gels	/	4			
	sample 11		/	6			

Based on the screening criteria of heat source power, contact surface roughness, and thermal conductivity of the interface materials, we selected 11 samples, including the aforementioned models of metal solder sheets, silicone pads, carbon fiber pads, and thermal conductive gels. Comparative performance experiments were conducted between these interface materials and traditional interface materials, utilizing both welding and pressing techniques. Using a constructed heat sink performance testing platform, we completed performance comparison experiments for each interface material.

After filling or coating the thermal interface materials listed in the table between the light source substrate and the heat sink substrate, we conducted performance tests on the thermal interface materials. The performance test data for the metal solder sheet samples are shown in the Fig. 4.

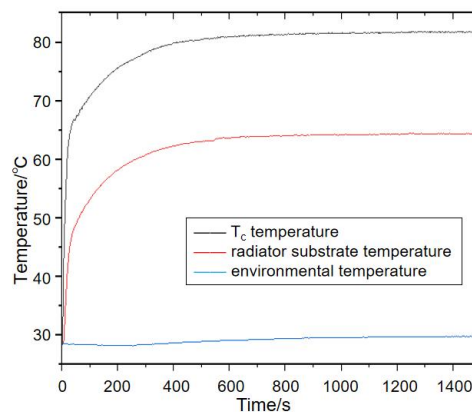


Figure 4. Temperature data of metal solder pad samples

The heat source power was set at 500W. Thermocouples were used to measure the temperatures at the solder joint of the heat source, the closest point on the heat sink base, and the ambient temperature, with readings taken every 5 seconds. To minimize measurement errors caused by the instruments during the temperature collection process, the final data for each point were taken as the average values obtained after the temperatures stabilized.

Based on the experimental data summarized, among the 11 samples of thermal interface materials tested, samples 3, 8, and 9 fail to meet the requirement for rapid heat transfer from the light source. This is attributed to the high surface roughness of both the light source substrate and the heat sink substrate, as well as the high hardness of the thermal interface materials. Consequently, when these thermal interface materials are sandwiched and fixed between the two substrates, they cannot completely fill the gaps between the substrates due to the presence of air pockets. This results in extremely low thermal conductivity at the thermal contact interface, causing a significant buildup of heat at the light source position once powered on. As a result, the generated heat cannot efficiently transfer to the heat sink substrate in a timely manner, adversely affecting the efficiency and lifespan of the light source. In severe cases, this can render the light source inoperable under high-power thermal dissipation conditions. Therefore, samples 3, 8, and 9 are not suitable for use in scenarios requiring high-power light source thermal management.

Sample 1 is a 0.1mm thick indium silver solder sheet, soldered using a reflow soldering process. Test results show that the temperature rise of the solder joint in Sample 1 is 74.8°C , whereas under the same conditions, traditional thermal interface materials experience a temperature rise of 50.5°C . Compared to traditional interface materials, Sample 1 exhibits an increased solder joint temperature rise of 24.3°C . Considering both performance and cost factors, it fails to meet the cooling requirements of the heat sink.

Sample 7 is a thermal pad with a hardness of 35 and a thermal conductivity of $8\text{W}/(\text{m}\cdot\text{K})$. After fixing the thermal pad between the heat source substrate and the heat sink substrate with screws for experimental testing, data indicates a solder joint temperature rise increase of 6.45°C compared to traditional thermal interface materials. Although Sample 7 meets the heat sink cooling requirements, its temperature rise is slightly higher compared to traditional materials, rendering its effectiveness less than ideal.

Sample 4 is a thermal pad with a hardness of 25 and a thermal conductivity of $6\text{W}/(\text{m}\cdot\text{K})$, exhibiting a solder joint temperature rise decrease of 0.2°C compared to traditional interface materials. Sample 5, with a hardness of 35 and a thermal conductivity of $6\text{W}/(\text{m}\cdot\text{K})$, shows a solder joint temperature rise increase of 1.85°C compared to traditional materials. Sample 6, featuring a hardness of 25 and a thermal conductivity of $8\text{W}/(\text{m}\cdot\text{K})$, shows a solder joint temperature rise increase of 0.7°C compared to traditional materials, indicating that Samples 4, 5, and 6 achieve interface filling and thermal conductivity results close to those of traditional interface materials.

Comparing sample 4 with sample 7, sample 7 exhibits higher hardness and thermal conductivity, whereas sample 4 shows lower hardness and thermal conductivity. However, experimental results indicate that sample 4 outperforms sample 7. This is attributed to the lower hardness of the thermal interface material in sample 4, which enhances its plasticity and filling capability. It better fills the gaps between the heat source substrate and the heat sink substrate, reducing air content. As a result, heat can rapidly transfer through the thermal interface material to the heat sink substrate, lowering the solder joint temperature.

Sample 2 is a 0.2 mm thick indium-silver solder, customized from sample 1 through improvements and adjustments. Compared to traditional thermal interface materials, sample 2 exhibits a 3.26°C reduction in solder joint temperature rise. Sample 11, with a thermal gel of $6\text{W}/(\text{m}\cdot\text{K})$ as a thermal grease, shows a temperature rise reduction of 2.34°C . These results demonstrate that both sample 2 and sample 11 possess excellent interface filling and thermal conductivity properties. They meet the gap-filling requirements between the light source substrate and the heat sink substrate and offer superior performance compared to traditional interface materials.

4. ADJUSTMENT AND IMPROVEMENT OF METAL WELDING LUG PROCESS

For metal solders, the process involves melting the metal material at high temperatures under pressure to bond the heat source substrate and the heat sink substrate together. During soldering, factors such as temperature and duration in each temperature zone, furnace environment during each phase, thickness of the metal solder, and thermal capacity of the heat source substrate and heat sink substrate all affect the soldering quality, thereby influencing the thermal transfer efficiency of the heat source.

Therefore, adjustments are continuously made to the temperatures, durations, and internal conditions of each temperature zone in the reflow soldering furnace based on the actual dimensions and conditions of electronic devices and the uniform temperature plate. After soldering is completed, industrial CT scans are conducted to inspect the soldering quality and perform quality testing.

The soldering process utilizes a heating stage and a reflow soldering furnace where gases circulate to generate high temperatures necessary for soldering. The process involves sequentially stacking the light source substrate, metal solder, and radiator substrate, and then pushing them into the reflow soldering furnace.

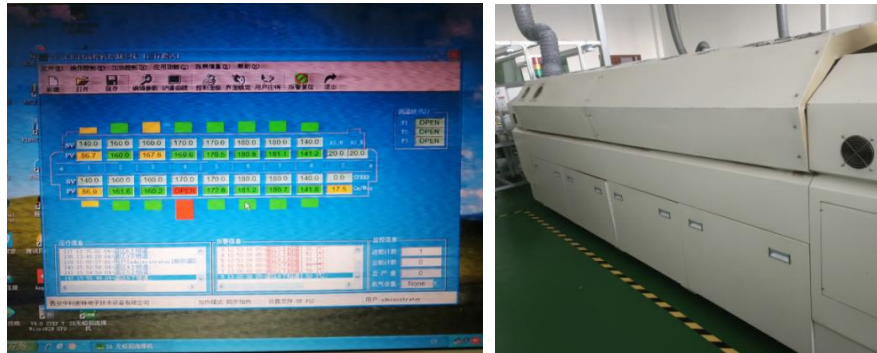


Figure 5. Reflow oven each temperature zone setting and reflow oven

The reflow soldering oven is divided into eight temperature segments across four zones: the heating zone, preheating zone, soldering zone, and cooling zone. As the heat source substrate-metal solder-heat sink substrate enters the heating zone of the oven, the metal solder softens, solvents and gases evaporate, and the flux within the metal solder wets the solder pad, causing the solder to soften, collapse, and cover the solder pad. Upon entering the preheating zone, the structure of the heat source substrate-metal solder-heat sink substrate is thoroughly preheated to prevent sudden exposure to the high soldering temperature that could damage the components. Moving into the soldering zone, the temperature rapidly rises, melting the solder paste, which wets, diffuses, and flows over the heat source and heat sink substrates, forming solder joints. Upon entering the cooling zone, the solder solidifies, completing the soldering process. The temperature adjustments of the soldering oven are illustrated in the Fig 5.

The integrated structure of the soldered heat source and heat sink substrate was subjected to industrial CT scan. Subsequently, it was pressed together with the main body of the heat sink to form the complete sample for performance testing. The welding quality was assessed using both industrial CT scan and heat sink performance testing methods. Based on the results obtained, adjustments were made to parameters such as welding furnace environment, duration, and temperature to optimize welding quality and performance. The welding process curve is shown in the following Fig 6.

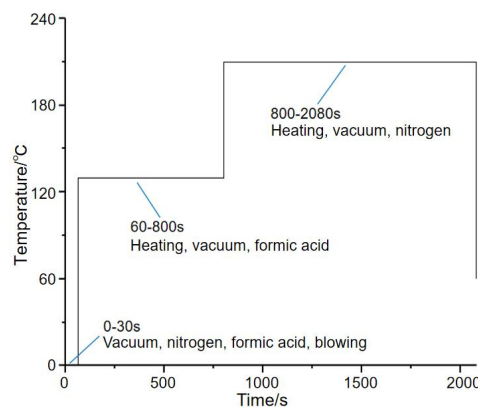


Figure 6. Welding process curve

After the initial experiments, industrial CT scans were used to validate the welding quality of the samples, revealing a porosity of approximately 50%. At this stage, the welding results were unsatisfactory as the metal solder struggled to efficiently transfer heat generated by the light

source to the heat sink, failing to meet the filling requirements of the contact interface and thus rendering them unusable. Following adjustments to the welding process and procedures, the samples were re-welded, resulting in significantly improved welding effectiveness. Thermal tests were subsequently conducted on the improved samples.

The experimental results indicate that, under 500W heating power, the heat sink achieved from the soldering process with the adjusted welding parameters showed a temperature rise of 53.9° C at the solder joint when filled with indium-silver solder, whereas the heat sink filled with traditional thermal grease showed a temperature rise of 57.2° C. Compared to samples filled with traditional thermal grease, the samples soldered with indium-silver solder exhibited a temperature rise reduction of 3.26° C at the solder joint, which closely matched the simulation results.

5. CONCLUSIONS AND RECOMMENDATIONS

Based on process adjustments and performance experiments on actual samples, and considering the overall aspects such as performance, cost, and process requirements of various thermal interface materials, the following conclusions and recommendations are drawn:

(1) For the 11 samples mentioned earlier, their performances were compared against traditional thermal interface materials based on temperature rise. Among them, samples 1, 3, 8, and 9 were found unsuitable for high-power light source thermal dissipation scenarios. Sample 7 exhibited poor performance. Samples 4, 5, and 6 showed performances similar to traditional thermal interface materials. Samples 2 and 11 demonstrated good interface filling and thermal conductivity, capable of meeting the gap filling requirements between the light source substrate and the heat sink substrate.

(2) When selecting thermal interface materials, thermal conductivity is not the sole consideration. Factors such as the thickness of the thermal interface material, surface roughness of the heat source and heat sink substrates, as well as the dimensions and thickness of these substrates, may all influence the selection and effectiveness of thermal interface materials.

(3) Compared with thermal conductive silicone greases, metal solders, thermal pads, and thermal conductive gels, thermal conductive gel solidifies after use, effectively securing and filling gaps between the heat source substrate and the heat sink substrate, demonstrating excellent stability. Metal soldering involves complex processes and relatively higher costs. It is suitable for situations where the surfaces of the heat source and heat sink are highly smooth, allowing for pressure bonding using metal soldering, thereby avoiding the complexities and high temperatures associated with this method.

6. Outlook

For electronic devices, as the prevalence of electronic equipment and the application of high-power electronic components increase, the power dissipation from heat sources and integration density continue to rise. This trend escalates the demand for thermal conductivity and heat dissipation effectiveness. Consequently, there is a growing need for thermal interface materials. In addition, the optoelectronic device industry presents significant market prospects and application demands for thermal interface materials that offer excellent fillability and high through-plane thermal conductivity.

REFERENCE

- [1] Chen H B, Chen R, Liu M Q, et al. Research progress of force-induced oriented highly thermally conductive polymer composites[J]. *Acta Materialiae Compositae Sinica*, 2022, 39: 1489-1500.
- [2] Li J, Ma C B, He T, et al. Analysis of applying high-power LED in the factory lighting[J]. *China Illuminating Engineering Journal*, 2011, 22(03): 43-48.
- [3] Xu Z. Study on gas-liquid two-phase motion mechanism and heat transfer characteristics of thermosyphon heat sink for LED cooling[D]. Harbin: Harbin Institute of Technology, 2018: 2-3.
- [4] Lin M T, Chang C C, Horng R H, et al. Heat dissipation performance for the application of light emitting diode[C]//Symposium on Design. IEEE, 2009: 145-149.
- [5] Ding C H, Zhang T Y, Luo J, et al. Optimization design research on high power LED lamps of radiator[J]. *Journal of Electron Devices*, 2016, 39(3): 750-754.
- [6] Yang G. Research on schemes about heat dissipation of high-power LED lamp in road lighting[J]. *China Illuminating Engineering Journal*, 2010, 21(01): 40-47.